J Comput Aided Mol Des (2009) 23:869–881
DOI 10.1007/s10822-009-9304-1

Comparative virtual screening and novelty detection for NMDA-Glycine$_B$ antagonists

Bjoern A. Krueger · Tanja Weil · Gisbert Schneider

Received: 8 June 2009 / Accepted: 1 October 2009 / Published online: 5 November 2009

Abstract Identification of novel compound classes for a drug target is a challenging task for cheminformatics and drug design when considerable research has already been undertaken and many potent lead structures have been identified, which leaves limited unclaimed chemical space for innovation. We validated and successfully applied different state-of-the-art techniques for virtual screening (Bayesian machine learning, automated molecular docking, pharmacophore search, pharmacophore QSAR and shape analysis) of 4.6 million unique and readily available chemical structures to identify promising new and competitive antagonists of the strychnine-insensitive Glycine binding site (Glycine$_B$ site) of the NMDA receptor. The novelty of the identified virtual hits was assessed by scaffold analysis, putting a strong emphasis on novelty detection. The resulting hits were tested in vitro and several novel, active compounds were identified. While the majority of the computational methods tested were able to partially discriminate actives from structurally similar decoy molecules, the methods differed substantially in their prospective applicability in terms of novelty detection. The results demonstrate that although there is no single best computational method, it is most worthwhile to follow this concept of focused compound library design and screening, as there still can new bioactive compounds be found that possess hitherto unexplored scaffolds and interesting variations of known chemotypes.

Keywords Drug discovery · *N*-Methyl-D-Aspartate receptor · Glycine$_B$ · Bayesian classifier · Pharmacophore · Novelty detection · Machine learning · Molecular shape · Docking · Structure–activity relationship

Introduction

The *N*-Methyl-D-Aspartate (NMDA) receptor is a member of the family of ionotropic glutamate receptors, and has been intensely studied for over two decades [1–5]. It is considered an attractive target for neurodegenerative disorders like Parkinson's [6] and Alzheimer's disease [7, 8], and Schizophrenia [9]. The NMDA receptor constitutes a hetero-tetramer complex [10] of different types of the subunits NR1, NR2 and NR3, which together form the ion channel [11]. The receptor is activated by the presence of both glutamate and glycine [12], where glutamate acts as the principal agonist and usually interacts with the NR2 subunit [13]. The co-agonist glycine binds to the strychnine-insensitive glycine binding site of the NR1 subunit (Glycine$_B$ site) [14]. Over-activation of the NMDA receptor results in excitotoxicity [15], thus suggesting the competitive antagonistic modulation (de-activation) of the Glycine$_B$ site to represent a desirable mode of action of a potential drug [16].

Electronic supplementary material The online version of this article (doi:10.1007/s10822-009-9304-1) contains supplementary material, which is available to authorized users.

B. A. Krueger · G. Schneider (✉)
Institute of Organic Chemistry und Chemical Biology,
Johann Wolfgang Goethe-University, Siesmayerstraße 70,
60323 Frankfurt, Germany
e-mail: g.schneider@chemie.uni-frankfurt.de
URL: www.modlab.de

B. A. Krueger (✉)
Merz Pharmaceuticals GmbH, Chemical R&D–Drug Design,
Eckenheimer Landstraße 100, 60318 Frankfurt, Germany
e-mail: Bjoern.Krueger@merz.de
URL: www.merz.de

T. Weil
Department of Chemistry, National University of Singapore,
3 Science Drive, Singapore 117543, Singapore

The increasingly limited availability of unclaimed chemical space and thus the lack of promising new starting points can be an issue in drug discovery projects [17]. In particular in their early phase "scaffold hopping" [18] is one of the most challenging objectives [19]. In this study, we performed a comparative application of several established computational techniques for virtual screening and library diversity analysis. We were interested to see whether identification of novel $Glycine_B$ antagonists ("novelty detection") is still possible by readily available virtual screening tools, even though the target has been the subject of many previous studies, and a significant numbers of potent ligands are already known.

Although the theoretical chemical space is considered to be immense [20, 21] the number of physically available compounds is approximately seven million, a quantity that has become feasible for ultra-high-throughput screening (uHTS) [22]. Due to the fact that HTS is a cost-intensive process [23] and hit rates of unfocused screening libraries are usually low [24], the concept of focused library design has received much interest [25–27]: Screening candidates are pre-selected, e.g. by cheminformatics methods, to enrich a library of compounds with potential actives prior to actual biochemical testing. Instead of screening large compound libraries by HTS, virtual libraries of available compounds are screened in silico, and only the virtual hits are actually tested for activity in vitro [28]. In this study, we mimicked this scenario, and compiled a collection of 4.6 million unique compounds from vendor catalogues as a source for potentially novel $Glycine_B$ antagonists.

Materials and methods

Preparation of reference and screening libraries

Library of reference actives

We performed a literature and patent search to collect reference molecules with a reported biological activity for the $Glycine_B$ site. Additionally, we searched for $Glycine_B$ antagonists in the chemical database WOMBAT 2007.2 [29]. As biological activities reported in publications or databases can deviate significantly for different biological assays or even laboratories, we decided to classify the retrieved compounds into three groups: *high affinity* ($IC_{50} < 1$ μM), *medium to low affinity* (IC_{50} above 1 μM but below 50 μM) and *inactive* ($IC_{50} \geq 50$ μM). 1,123 compounds were retrieved, from which 754 had a precise activity annotation. 429 compounds were reported to be nanomolar (*high affinity*), and 288 still had a reported $IC_{50} < 50$ μM (*medium to low affinity*). 37 compounds were classified as inactive.

Library of screening compounds

8.8 million commercially available chemicals originating from 46 different supplier catalogues were collected as screening compound pool. We applied stringent filters to discard "unwanted" compounds, that is, molecules with a high probability of causing safety alerts or other undesirable molecular features which would hamper their later development. First, a REOS [30] filter and a filter according to Hann et al. [31] were implemented using SMARTS [32, 33] pattern matching in SciTegic Pipeline Pilot 6.1.5 (Accelrys Inc., www.accelrys.com) to remove molecules with unwanted substructures, e.g. known toxicophores or molecular features known for creating false-positives in screening assays. Then, a filter according to Lipinski's Rule of Five [34] was applied. While an unconditional application of Lipinski's rule of five is not always desirable [35], we decided to apply a more "softer" version, allowing for the violation of up to one of the rules of five, in order not to exclude too many potentially interesting compounds. All remaining molecules were "washed" (ions were removed, remaining structures neutralized, stereo chemistry standardized) using the protocol "Standardize Molecule" available in Pipeline Pilot. After a redundancy check, 4,580,603 unique structures in two-dimensional annotation were retained with average values for molecular weight of 390 (± 74.5), AlogP of 3.5 (± 1,5), number of hydrogen bond donors of 1.1 (± 0.8), number of hydrogen bond acceptors of 4.4 (± 1.6), and mean number of rings within the molecules of 3.3 (± 1.0).

The software tools LigPrep 2.2 and Epik 1.6 (Schrödinger, LLC, New York, 2008) were used for computing probable protonation states at pH 7 ± 3, all tautomers, and up to 32 stereoisomers for compounds containing unassigned stereocenters. A total of 11,405,564 isomeric forms were computed from 4,580,603 two-dimensional molecular structures. In order to comprehensively sample 3D space, up to 250 conformers were generated for each of the isomers using Phase 3.0 (Schrödinger, LLC, New York, 2008). Conformers with *rmsd* < 1 Å to an existing conformation of the same molecule were discarded. After minimization and redundancy checks, 751,223, 292 conformers were stored in several Phase conformer databases for virtual screening.

Library diversity analysis

In order to assess the chemical diversity of both reference actives and virtual screening hits, a classification of the different chemotypes present in the respective libraries was performed using the "cluster molecules" function in Pipeline Pilot. The maximum dissimilarity algorithm [36] was used. As a modification to the original algorithm,

re-centering was allowed twice during clustering to minimize the maximum distance between cluster centers and reduce the impact of potential structural outliers, e.g. singleton molecules. Intermolecular distances were calculated as topological Tanimoto similarity Eq. 1 of functional connectivity fingerprints (FCFP-6) as implemented in Pipeline Pilot.

$$T = \frac{c}{a + b - c}, \tag{1}$$

where a are the bits set to "1" in molecule A, b are the bits set to "1" in molecule B, and c are the "1" bits common to both molecules. Tanimoto similarity T ranges from zero (maximum pair-wise dissimilarity) to one (identity).

Receiver-operating-characteristics (ROC) [37, 38] plots were generated as a means of assessing the classification power of the computational models. Here, sensitivity is plotted against specificity. Sensitivity and specificity are calculated by the corresponding number of true positives (TP), true negatives (TN), false positives (FP) and false negatives (FN) Eq. 2.

$$\begin{aligned} \text{Sensitivity} &= \text{TP}/(\text{TP} + \text{FN}) \\ \text{Specificity} &= \text{FN}/(\text{FP} + \text{TN}) \end{aligned} \tag{2}$$

Matthews' correlation coefficient [39] Eq. 3 represents an additional means of scoring the sensitivity and specificity of a classification method. Its score ranges from -1 (anti-perfect model) to $+1$ (perfect model) while 0 corresponds to a random classifier.

$$MCC = \frac{TP \cdot TN - FP \cdot FN}{\sqrt{(TP + FP)(TP + FN)(TN + FP)(TN + FN)}}, \tag{3}$$

where TP is the number of true positives, TN true negatives, FP false positives and FN false negatives.

2D virtual screening methods

Laplace-modified naïve Bayesian classifier

The concept of Bayesian statistics has been successfully applied in various research areas [40]. Recently, it has received increasing interest as a tool for drug design [41–45]. The conceptual simplicity and human interpretability of a Bayesian model makes this method an attractive tool for evaluating structure–activity-relationships (SAR) of a given set of ligands [45, 46]. We applied the concept of the Laplace-modified naïve Bayesian classifier as implemented in Pipeline Pilot 6.1.5 by calculating the functional connectivity fingerprints (FCFP-6) of all reference Glycine_B ligands from literature marked as "good" and presenting them to the model together with decoy molecules marked as "bad". The classifier "learned" by calculating the frequency of occurrence of "good" molecular features vs. the background noise of the inactives. The score of a molecule is generated by calculating the individual molecular features of the sample and summing up the Laplacian-adjusted weights of each feature to form a probability value. This score thus represents a relative likelihood of the given molecule to be originating from the subset of "good" molecules.

Four different Bayesian models were trained. To assess the principal classification power of a naïve Bayesian model, we did not differentiate between *high affinity* and *medium to low affinity* reference actives in a first approach. The principal idea was that while highly active structures should be enriched with few characteristic molecular features or substructures desirable for biological activity (and thus receive a high probability of activity), substructures present in *medium to low affinity* compounds should be more diverse and their individual occurrence more rare (thus only receiving low probabilities of activity).

As a retrospective validation for the first model, all 1123 reference structures compiled from literature, patents and biological databases were divided into 20 clusters using the maximum dissimilarity algorithm on the FCFP-6 molecular descriptor. We separated four clusters (73 structures) with the highest mean distance of their individual cluster center (compounds **1**–**4**) to all other molecules into an external validation set. This set was never used during model generation. The remaining 1050 reference compounds were used for model training (Bayesian model 1). An additional set of physicochemical descriptors (AlogP, number of hydrogen bond donors and acceptors and the number of rotatable bonds) was used for the training of Bayesian model 2 to assess if the model's predictive power would profit from further information about the molecules (Fig. 1).

All molecules present in the WOMBAT database excluding compounds with annotations specifically for our target of interest (Glycine_B) were collected as decoy molecules. Ligands for other subunits of the NMDA receptor like NR2A were included as decoys to enhance the NMDA subunit selectivity of the model. Subsequently, the previously defined drug-like and garbage filters were applied. A 50% random split was performed, summing up to 61,291 and 61,221 decoy molecules for the training and external test set, respectively.

In an additional approach, a second Bayesian model was trained solely on compounds with annotated nanomolar activity as reference actives (416 structures), while structures with reported activity higher than 30 μM were added to the previously compiled set of decoy molecules (Bayesian model 3). We thereby evaluated if it is not only possible to classify between potentially active and inactive molecules for a given target but also to specifically predict nanomolar affinity. The actives were divided into six

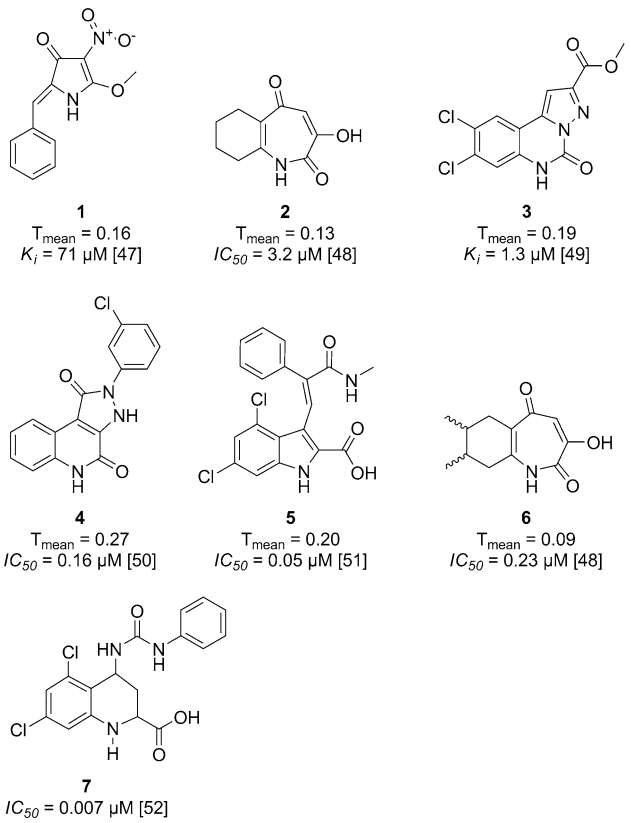

Fig. 1 Structures 1–6: cluster centers of the external test sets, their mean similarity to all other molecules in the test set (Tanimoto similarity, FCFP-6 fingerprint) and reported in vitro affinities. Structure **7**: Reference molecule for 3D shape search

clusters. Two (54 structures, cluster centers **5** and **6**) were separated into the external test set, while the structures in the remaining four clusters (363 structures) were used for model training. The same setup was used to evaluate the effect of additional physicochemical descriptors (AlogP, number of hydrogen bond donors and acceptors and the number of rotatable bonds) on the model's predictivity (Bayesian model 4).

After model calibration, a prospective virtual screen was performed on our screening library of approx. 4.6 million unique commercially available compounds in two-dimensional atomic annotation.

3D virtual screening methods

Molecular docking into a rigid receptor

Several crystal structures of the extracellular binding domain of NR1 ($Glycine_B$ site) have been published and deposited in the protein data base [53] (PDB). Mainly the crystal structures of NR1 with the agonists glycine [54] (PDB code 1PB7), D-serine [54] (1PB8), the partial agonists D-Cycloserine [54] (1PB9), ACPC [55] (1Y20) and ACBC [55] (1Y1Z) and the antagonists Dichlorokynurenic acid [54] (DCKA–PDB code 1PBQ) and Cycloleucine [55] (1Y1M) are of interest due to their high resolution of 1.9 Å and below. We chose the crystal structure of NR1 in complex with DCKA since DCKA is the largest ligand in the series and thus the binding site is the bulkiest of the antagonistic ones [54]. The different crystallization studies of NR1 showed that the $Glycine_B$ site is able to accommodate ligands of different molecular size [11, 54, 55], and thus, a distinct amount of induced receptor flexibility is discussed in the literature [56, 57]. Also, the larger size of several reference actives more potent than DCKA indicates that NR1 is able to bind potent voluminous ligands. We performed docking experiments with a limited implementation of receptor flexibility. Both the vdW-radii of ligand atoms and atoms of the different protein side chains in the binding site were allowed to be scaled down to 70% to reduce potential clashing between ligand and receptor atoms. We defined the $Glycine_B$ binding site to be consisting of all amino acid residues within a range of 12 Å of the geometric center of the co-crystallized ligand DCKA in the crystal structure of NR1 (PDB ID 1PBQ).

The crystal structure 1PBQ was prepared using the Protein Preparation Wizard as implemented in the Schrödinger 2008 Suite: explicit hydrogens were added to the protein residues, bond orders were assigned, and crystal waters were removed. The likely tautomerization states of the binding site residues were calculated, and finally, the protein was subjected to a short force field relaxation in the OPLS2001 force field [58] to an RMSD of 0.18 Å in order to remove unresolved clashes. To test whether this structural modification has an impact on the enrichment rate, we performed docking experiments both with a force-field minimized and the original receptor (unmodified coordinates from the crystal structure). Molecular docking was carried out using Glide SP [59, 60] and Glide XP [61] (Glide, version 5.0, Schrödinger, LLC, New York, 2008).

In a first validation, we tested the enrichment rate of the docking approach using 416 nanomolar actives hidden within a decoy set of 4427 inactives using Glide SP. The decoys were chosen by 2D similarity search (FCFP-6 descriptor, Tanimoto similarity, Pipeline Pilot) using all high-affinity reference actives as query structures. The search was performed in the WOMBAT database, having removed all compounds with known activity on $Glycine_B$. The application of decoys similar to the active structures is considered to be a more "challenging" validation than random sampling [62] because it increases the difficulty for the docking and scoring algorithms to discriminate actives from the very similar inactives.

A second validation was performed using the enhanced scoring function of Glide XP to eliminate potential false

positives due to more rigorous scoring [61]. In a third and final validation, we assessed the impact of docking with receptor constraints on the quality of the results. Four docking constraints were defined as they have been described as crucial interaction points in the binding site [54]: Hydrogen bond (H-bond) formation to the residues Arg523, Pro516 and Thr516 and a hydrophobic area at the location of the aromatic ring system of co-crystallized ligand DCKA. While H-bond formation is crucial for the actual binding affinity, pi-stacking interaction between the ligand and Phe484 is considered to be essential for antagonistic activity [55]. During docking, at least three of these four constraints had to be fulfilled; otherwise a ligand pose was discarded.

Following up on the validation, we performed prospective molecular docking for a subset of compounds (exhaustive docking would have been rather time-consuming), summing up to 3,076,242 isomeric forms in three-dimensional atomic annotation originating from 1,413,733 unique structures in 2D. The subset selection was based on immediate commercial availability of the compounds.

3D pharmacophore hypothesis and QSAR model

Using the 194 most active (nanomolar) literature ligands as reference compounds, a 3D pharmacophore hypothesis was generated using Schrödinger Phase 3.0. We used molecular clustering to create an external test set. Two structural clusters were separated and not used as training data. The pIC_{50} was calculated for each ligand and an activity cutoff of $pIC_{50} = 8.5$ was set to define actives. Ligands with an activity of $pIC_{50} = 6$ and below were considered inactives. To generate 3D conformers for training and validation of the created QSAR models, ConfGen version 2.0 (Schrödinger, LLC, New York, 2008) was used to sample a maximum of 100 steps per rotatable bond and up to 1,000 conformers were generated per compound. Sampling was set to "thorough", and pre-minimization (maximum 100 steps) and post-minimization (up to 50 steps) were applied to minimize the conformers' energies. All minimizations were computed within the OPLS2005 force field with an implicit GB/SA water solvation treatment. Redundant conformers were eliminated using an RMSD cut-off of 1 Å. We decided not to define any excluded volumes to avoid bias of the purely ligand-based approach with structural data from a possible flexible receptor structure.

Different pharmacophore hypotheses were generated and retrospectively validated. We chose the model with the highest predictive power as a pharmacophore hypothesis for subsequent virtual screening. Additionally, a QSAR model was built on the chosen pharmacophore hypothesis and its predictive power was validated as implemented within Schrödinger Phase. Here, the molecules to be scored were aligned to the pharmacophore hypothesis. A rectangular grid was defined around the ligands and equally divided into cubes of 1 $Å^3$ size. Then a regression analysis by Partial Least Squares (PLS) [63, 64] was performed, where the binary-valued occupancies of these cubes by the ligands' atoms acted as independent variables and the ligands' activities as dependent variables. Spatial occupancy of a cube was deemed to occur if the cube's center fell within the atom's van der Waals radius. The QSAR model's performance was then assessed on the previously compiled external test set.

Finally, prospective virtual screening was performed on our precomputed 3D database containing approx. 751 million conformers.

3D shape search

The analysis of the volume of a molecule, preferably in its biological conformation, is an additional concept for virtual screening of molecules that has been receiving growing attention in the drug design literature lately [30, 65, 66]. We used the structure of the low nanomolar compound [67] **7** as a reference for a 3D shape search applying Schrödinger's Phase. The probable isomerization state was assessed at pH 7.4 using Epik 1.6 and the corresponding 3D structure was energy-minimized using MacroModel 9.6 (Schrödinger, LLC, New York, 2008) (OPLS2005, Generalized Born implicit solvent model, constant dielectric treatment of 1.0 and gradient-descent convergence after 1,000 iterations).

As a validation of the method, we virtually screened our compiled test set of ligands and exploited different shape representations with increasing information content as search parameter: pure molecular shape (simple volume as defined by the vdW radii of the ligand atoms), shapes of elements (vdW radii of ligand atoms, encoded with their corresponding chemical element), shapes of pharmacophores (vdW radii of ligand atoms, encoded with their corresponding pharmacophore type) and shapes of electrostatics (vdW radii of ligand atoms, encoded with their corresponding force field type according to MacroModel). This study provided us with the information which atom type representation distinguished best between $Glycine_B$ actives and decoy molecules according to molecular shape. The chosen atom typing was subsequently used in a prospective virtual 3D shape screening of our 751 million conformer database.

Results and discussion

2D virtual screening

Bayesian classifier

Different Bayesian classifiers were trained and retrospectively validated. In a first approach, we evaluated if

classification of molecular structures alone is sufficient to discriminate between actives and decoys. The performance of a model trained on the molecules' functional connectivity fingerprints (FCFP-6) was compared to the predictive power of a model trained on FCFP-6 plus a number of additional descriptors like AlogP, number of H-bond donors and acceptors and the number of rotatable bonds. In this model, all 1,123 literature references were used for testing.

The same approach was followed for a second comparison. Here, we selected only nanomolar reference compounds as actives during training (347 structures), while literature references with an IC_{50} above 30 μM were added to the decoy set. The predictive power of all four Bayesian models were evaluated using an external test set with molecules (both actives and decoys) never presented to the system as described in the methods section. The quality of the different results was analyzed using ROC plots (Fig. 2).

We found that while using reference actives with all ranges of reported activities, molecular structure provides already sufficient information to discriminate $Glycine_B$ ligands from decoy molecules. Even though there was a notable difference in internal model validation quality (Table 1), further training data features like AlogP or number of rotatable bonds did not extensively alter the result for the external training set. It was also apparent that a validation using an external test set shows a more "realistic" result compared to relying solely on the over-optimistic internal cross-validation of the model building process, represented as the Area-Under-the-ROC-curve (AUROC). We thus additionally calculated the corresponding Matthews correlation coefficient for all models to have a better estimation of prediction quality.

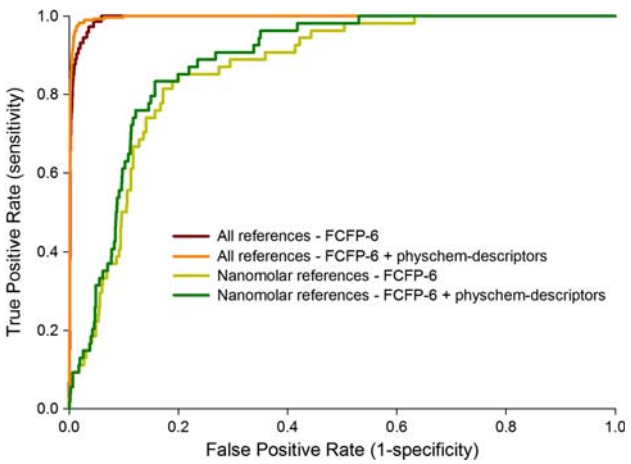

Fig. 2 ROC plot of four different Bayesian classifiers: all reference ligands (Bayesian model 1), all references plus additional physicochemical descriptors (model 2), nanomolar-only references (model 3) and nanomolar-only references plus additional physicochemical descriptors

Table 1 Internal and external validation of different Bayesian classifiers: model 1 (all reference structures, FCFP-6 descriptor), model 2 (all reference structures, FCFP-6 plus additional physicochemical descriptors), model 3 (only nanomolar reference structures, FCFP-6) and model 4 (nanomolar reference structures, FCFP-6 plus additional physicochemical descriptors)

Bayesian model	Internal validation		External validation MCC
	AUROC	MCC	
1	0.99	0.67	0.47
2	0.99	0.80	0.56
3	0.99	0.60	0.34
4	0.99	0.61	0.37

A different outcome was apparent for the "nanomolarity" prediction model. Here, the model was poorly capable of identifying unknown nanomolar $Glycine_B$ antagonists originating from the external test set. A reason for this finding might be the increased "fine graining" of training and test data: the number of structures available for statistical analysis is reduced compared to the first model, and the chemotypes are now divided into fewer, yet more separated clusters. As a consequence, the Bayesian classifier is supplied with less information. Still, this model was able to identify approx. 50% of unknown nanomolar actives within the first 10% of the test set. Notably, adding more properties for learning did not increase the model's classification power (Table 1).

We applied the classifier with the highest predictive power (model 2) to virtual screening of a previously prepared vendor library. 4.3 million molecules were analyzed, out of which 35,756 structures were predicted as actives by the Bayesian classifier. The top 500 compounds ranked by the Bayes-score were saved in a preliminary hit list for subsequent manual selection.

Both the model generation and application during virtual screening were highly time-efficient. Training of a Bayesian classifier with 1,023 actives and approx. 60,000 decoy molecules took less than 3 min on an Intel Xeon CPU with 2.33 GHz. Prospective virtual screening of the complete vendor library consisting of 4.6 million unique structures in 2D representation took approx. 20 min on the same CPU, analyzing up to 200,000 molecules per second.

3D virtual screening

Molecular docking

The retrospective enrichment of different docking and scoring algorithms and the effect of setting docking constraints were assessed using the previously compiled docking validation set. Also, we validated the effect on using an energy-minimized receptor structure in comparison with the

original crystal structure as deposited in the PDB. We found that while all methods performed reasonably well and produced near-identical high enrichment rates (*cf.* supplementary information, S1), there were some smaller differences in quality. In the overall set, the ranking of actives generated a better enrichment for Glide SP than the presumably more precise Glide XP. Docking into an energy-minimized receptor structure produced better results than for the original crystal structure. The use of docking constraints seemed not to have a substantial impact on the enrichment results for Glide SP, while using Glide XP with no constraints produced even slightly better results than with constraints. Glide XP with constraints produced the least optimal enrichment curve in the enrichment set. Still, the overall results for the complete set of ligands were very comparable.

We analyzed the enrichment in the best 300 structures ranked by docking score (Fig. 3). In this case, a more differentiated picture could be observed: While the use of Glide SP with constraints (energy-minimized and original receptor structure) showed the best receiver-operating-characteristics, Glide SP with no constraints produced the worst overall result in this data set. Also, the use of constraints resulted in an increasing recall rate for Glide XP.

We then tested if the application of the "Virtual Screening Workflow" as integrated in the Schrödinger 2008 Suite has an impact on the quality of prediction. Here, different docking stages were performed sequentially: Ligands which pass an initial "high-throughput virtual screening" (HTVS) step were subsequently analyzed in Glide SP and finally Glide XP. Each step applied a more sophisticated scoring, starting from rapid analysis with the HTVS scoring function, which has a much more restricted conformational sampling than Glide SP and is basically a crude assessment of ligand-receptor shape complementarity. Since the number of ligands which were passed on was

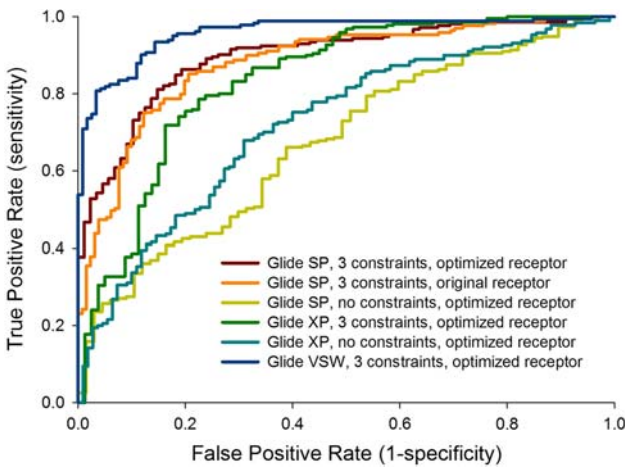

Fig. 3 ROC plots for the best 300 hits ranked by docking score. Results for Glide SP without constraints were identical for the optimized and non-optimized crystal structure

significantly reduced (by default, only the best 10% of structures reached the next level), the computational time needed to screen large ligand sets was substantially decreased compared to a full Glide SP or Glide XP run.

We found that all algorithms tested in this study were able to successfully dock different numbers of ligand molecules, e.g. Glide XP produced considerable fewer docking poses than the "softer" Glide SP (Table 2). We again calculated the Matthews correlation coefficient for all docking runs to additionally quantify the prediction correctness. In total, 282 actives and 4,386 decoy molecules were to be docked by the different algorithms.

The poorest enrichment was obtained with the "forgiving" scoring function of Glide SP without setting docking constraints: the result was only slightly better than a pure random selection because the algorithm produced docking poses for nearly all decoy molecules. The introduction of constraints improved the situation only to some extent: we still obtained near-random enrichment, while the amount of false positives (decoys for which docking poses were calculated) was decreased by approximately 50%. The use of the more strict scoring function somewhat improved the situation: while Glide XP with no constraints docked nearly all false positives, the introduction of constraints resulted in an acceptable Matthews CC of 0.47.

It was apparent that all methods produced a considerably better enrichment within the best 300 poses ranked by docking score. Using Glide SP with and without constraint and Glide XP with constraints, the best enrichment was achieved. We observed the performance of Glide XP and SP without constraints to be slightly worse for the original crystal structure than with an energy-minimized receptor. It is worthwhile to notice that the computationally less demanding results from the Schrödinger "Virtual Screening Workflow" showed a comparable enrichment rate to all methods which required ten times or more the amount of computational time.

As a conclusion from these preliminary experiments, we decided to further employ Glide SP with docking constraints for prospective virtual screening.

3D pharmacophore searching

88 different pharmacophore hypotheses were generated by a superposition of a maximum of seven and a minimum of five pharmacophoric points of the 194 potent $Glycine_B$ reference ligands using Phase 3.0. We chose the model with the best predictive power (defined by the Phase selectivity score) as a pharmacophore query for external validation and subsequent virtual screening (Fig. 4). The model also fitted the structural constraints postulated for the interactions of $Glycine_B$ ligands formed within the $Glycine_B$ binding site as suggested by molecular docking.

Table 2 Number of actives and inactives docked and the corresponding quality of prediction (Matthews' correlation coefficient–MCC) for the complete set of docked ligands and the best 300 ligands ranked by docking score

Model	Complete set			Best 300 poses		
	Actives docked	Inactives docked	MCC	Actives docked	Inactives docked	MCC
Glide SP, no constraints, original crystal structure	232	4,050	0.06	190	70	0.76
Glide SP, no constraints, optimized crystal structure	232	4,230	0.04	197	67	0.78
Glide SP, 3 constraints, original crystal structure	165	1,278	0.20	151	131	0.57
Glide SP, 3 constraints, optimized crystal structure	195	1,434	0.23	188	88	0.73
Glide XP, no constraints, optimized crystal structure	218	3,987	0.02	161	110	0.62
Glide XP, 3 constraints, optimized crystal structure	206	501	0.47	189	80	0.74
VSW using Glide SP, 3 constraints	–	–	–	182	118	0.67

A QSAR model was built for the chosen pharmacophore hypothesis by Partial Least Squares analysis of the occupancy of 3D space by the pharmacophoric points of a ligand as implemented in Phase 3.0. A first validation on internal test data (50% scrambling of actives and inactives to produce trainings and test sets) showed the QSAR model to produce a promising predictivity with $R^2 = 0.75$ and $Q^2 = 0.59$ using three PLS factors.

During validation using the external test set, we noticed that the use of the QSAR model produced a considerably better enrichment than the Phase fitness score alone (Fig. 5). Using the Phase fitness score, one half of our external test set was recognized immediately, the other half was ranked randomly or even anti-correlated. Further analysis showed that these molecules originated from different series, so the displacement was not scaffold-specific. Even though the molecules matched the pharmacophore of our query hypothesis, the Phase vector term of the misplaced ligands, a part of the Phase fitness scoring function, differed notably from the vector scores of the actives identified by the model (data not shown). Since the Phase vector score added a term for the directionality of e.g. H-bonds, we assume that the molecules were incorrectly classified due to mismatches in the conformer sampling. We decided not to weigh down the vector term in the Phase fitness function but instead to apply the QSAR model as scoring function for prospective virtual screening of our prepared databases of 751 million energy-optimized non-redundant conformers. After several days of calculations on a 26 CPU cluster, the 500 best compounds according to QSAR scoring were saved in a preliminary hit list and subsequently inspected visually.

3D shape search

In a final experiment, we applied 3D shape search as implemented in Phase to screen for novel Glycine_B antagonists. Since Phase offers different options for atom typing (pure volume–no atom typing at all, elemental, pharmacophoric or MacroModel (force field) atom typing), we first validated which atomic representation would produce the best retrospective results. A retrospective shape

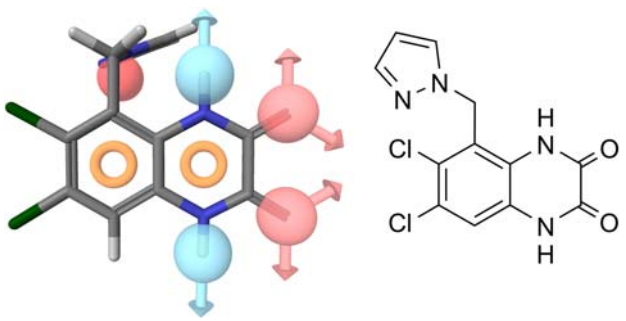

Fig. 4 Pharmacophore hypothesis (*left*) with the highest predictive power for the external test set with three-dimensional superposition of reference ligand [68] (*right*). *Brown rings* aromatic; *blue spheres with arrows* H-bond donors plus direction of potential H-bonds; *red spheres with arrows* H-bond acceptors plus direction of potential H-bonds; *dark red sphere* negatively ionizable

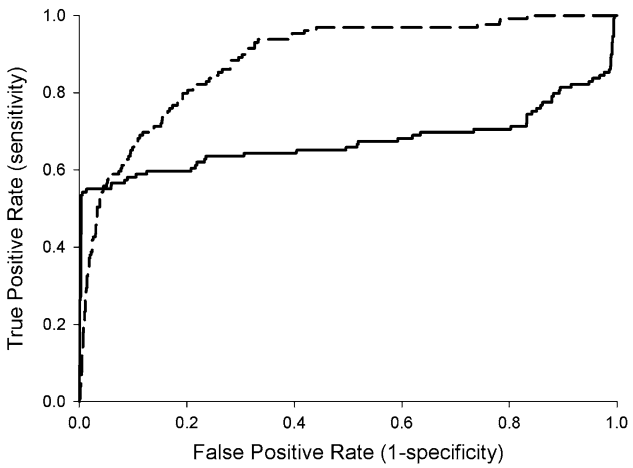

Fig. 5 ROC plots of the pharmacophore searches using fitness (*solid line*) and the QSAR model (*dashed line*) as scoring functions

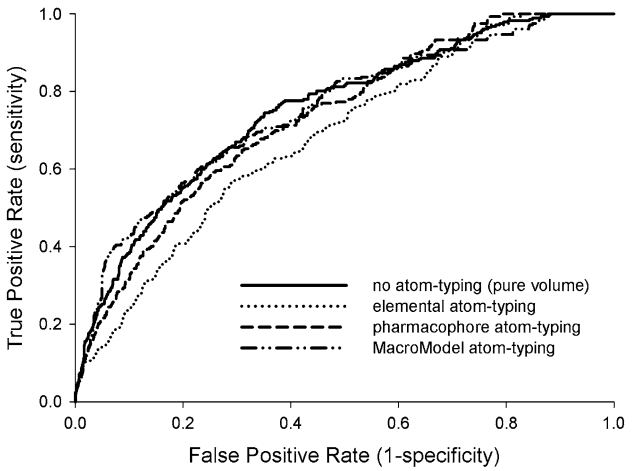

Fig. 6 ROC plots of different scoring mechanisms for shape-based similarity searching

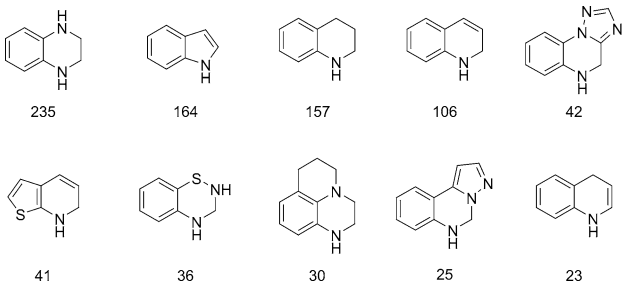

Fig. 7 Ten most frequent scaffolds present in the $Glycine_B$ literature references and their absolute frequencies of occurrence

search using the defined query structure of reference ligand **7** was performed with the previously compiled external test set.

We found that force-field atom typing together with no atom typing at all (pure volume) produced a better enrichment rate than e.g. elemental or pharmacophoric atom coding (Fig. 6); we thus decided to perform shape screening with MacroModel atom typing. Generally, the retrieval rate of actives was considerably reduced compared to other methods which were applied during this study. It might be argued that shape in itself, even with specific atom typing, is insufficient for discrimination of $Glycine_B$ antagonists from inactive decoy molecules. Still, the parallel application of multiple, diverse reference shapes with subsequent unified ranking ("consensus-shape") did not provide us with a significantly better result (data not shown). We thus decided to generate a reduced list of 100 preliminary virtual hits which were then visually inspected in order to weigh down the impact of this method on the final results.

Novelty analysis

For an assessment of the novelty of the identified hit molecules, we analyzed the set of $Glycine_B$ antagonists for frequently occurring molecular fragments by isolating their continuous ring assemblies ("Generate Fragments" in Pipeline Pilot 6.5) and counting their corresponding frequency of occurrence. The 10 most frequent ring systems were considered as "not novel" and saved in a list of known scaffolds (Fig. 7). At total, a number of 91 unique continuous ring systems were identified.

For each virtual screening method applied, we performed a substructure search for those scaffolds and removed any compound from all lists of virtual hits that contained a known scaffold. Only the most simple ring systems like benzene, cyclohexane, naphthalene etc. were kept so that we gained a list of molecules with scaffolds that–to the best of our knowledge–have not been comprehensively described for $Glycine_B$ activity. We also kept structures which contained a known scaffold but were considered to be of interest, e.g. because of novel structural variations like an additional cyclic substituent. Although the exclusion of scaffolds with known activity on the target might have reduced the hit rate of this study, we wanted to aim our experiments on novelty assessment (that is, dissimilarity to known reference structures (cf. Supplementary Information, S2)). The best 500 structures identified by each method were selected according to the individual scoring method and merged. Finally, this list was visually inspected, and 201 molecules were cherry-picked for ordering and testing.

In vitro screening results

The candidate compounds were evaluated in an in vitro binding assay testing the displacement of the reference compound MDL-105,519 [69] in an automated setup. A first preliminary screening was done by single-point evaluation, and only the more promising compounds were re-tested with full dose–response-curves. We found that the screened substances showed a wide array of binding affinities, most of them in the low-to-medium micromolar range (44 compounds with an estimated IC_{50} below 100 μM). While compounds with a micromolar affinity may not be considered to be lead structures for subsequent preclinical development, they can act as starting structures for further synthesis and optimization. Also, many of the resulting screening hits were rather fragment-like, e.g. of low molecular weights making these structures valuable targets for further chemical modifications. We selected some of the identified hits that are rather "atypical" and possess potentially new scaffolds (compounds **10** to **27**), although not all hit structures can be shown here due to proprietary considerations. While the screening hits **8** and **9**

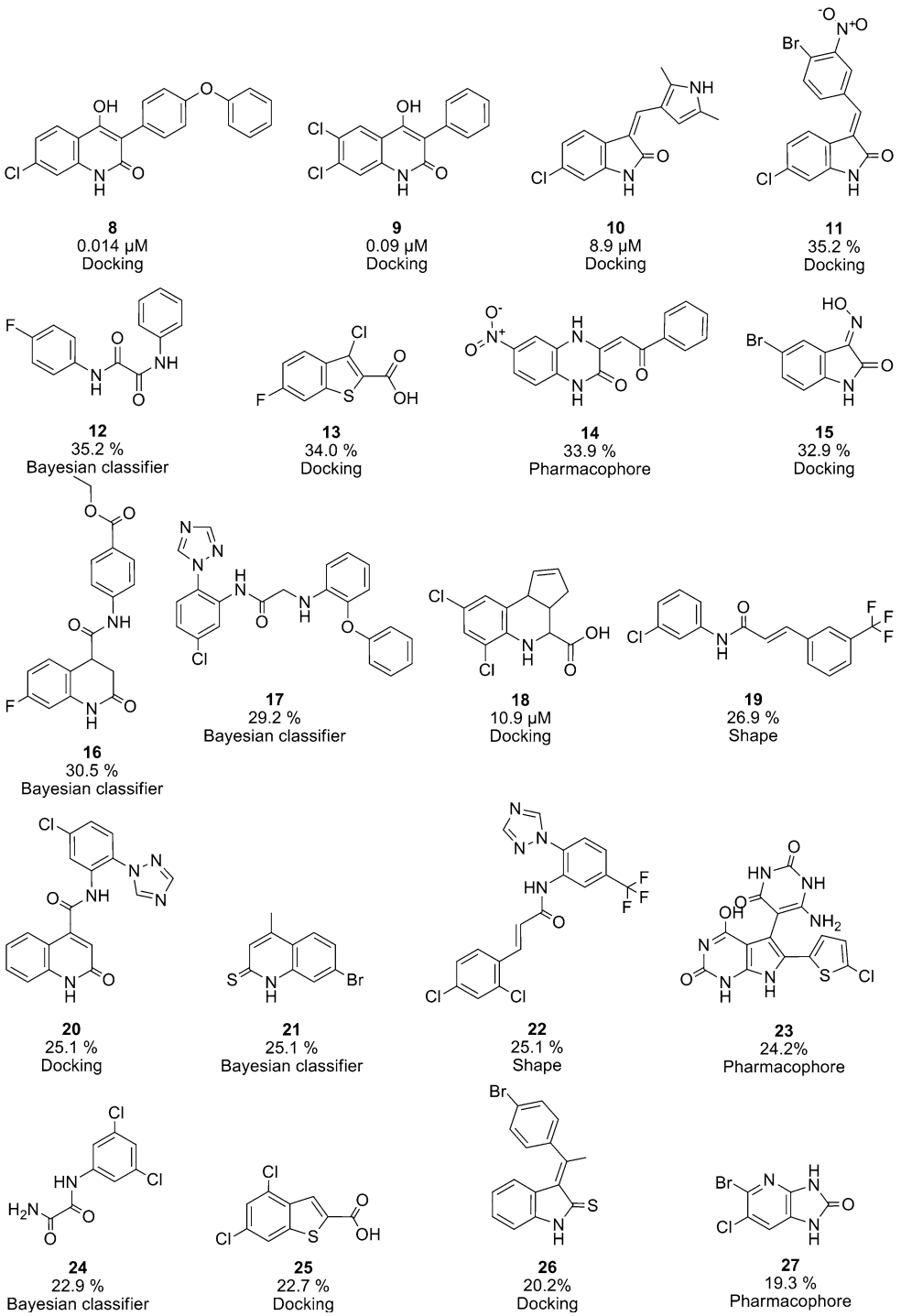

Fig. 8 Selected Glycine$_B$ hits and their corresponding in vitro IC_{50} value (in μM) or percent inhibition at 10 μM concentration, respectively. Also annotated is the computational method used to identify the compounds

represent analogues of literature references with known scaffolds, they have been included here to demonstrate that low nanomolar hits can be identified by the methods applied in this study (Fig. 8).

We found that all virtual screening methods used in this study provided us with reasonable numbers of novel bioactive compounds; the percentage of molecules with known scaffolds ranged between 12 and 35% (Table 3). An evaluation of random enrichment with known scaffolds by 10-times random selection of 500 structures from each method's validation set showed an average of 32.9 ± 1.9% known scaffolds. Molecular docking identified the fewest novel structures, and a high enrichment with known Glycine$_B$ scaffolds was observed within the 500 best-ranked

Table 3 Performance of different virtual screening methods concerning computational time, novelty detection as number of known scaffolds in the corresponding method's best 500 results, acceptance by human experts and actual in vitro activity

Method	Computational time required	Structures processed	Known scaffolds within best 500 hits	Expert-selected hits	Compounds with in vitro activity ($IC_{50} < 100$ μM)
Bayesian classifier	30 min	4,580,603	85 (17%)	12 (6%)	6 (3%)
Docking	56 days	3,416,705	175 (35%)	42 (21%)	22 (11%)
Pharmacophore	130 days	751,223,292	60 (12%)	107 (53%)	12 (6%)
Shape	104 days	751,223,292	75 (15%)	40 (20%)	2 (1%)

The computational time required was standardized to 1 CPU since different amounts of CPUs were employed for each method. Percentages in expert-selected hits and compounds with in vitro *affinity* are taken from the total number of tested virtual hits (201 compounds)

docking results (35%). The Bayesian classifier, pharmacophore and shape search showed more scaffold-hopping potential with 17%, 15% and 12% enrichment with known scaffolds, respectively, which is substantially below the average random enrichment of 32.9%. Also, the methods differed considerably in their ability to identify potent hits: While the number of actives retrieved by docking and pharmacophore searching was acceptable, shape analysis performed significantly worse. The Bayesian classifier correctly predicted six of nine tested compounds which were picked by the human expert.

Additionally, we tried to estimate the impact of "cherry picking" by human experts on the quality of the results in terms of actual in vitro affinity of the selected compounds. We found one of the possible reasons for the low percentage of expert-accepted hits from the Bayesian classifier to be the structural composition of the virtual hits themselves. After having removed compounds with known scaffolds, many compounds like **12** and **24** were enriched in the refined hit list. While they partially consisted of molecular substructures of known $Glycine_B$ antagonists, the spatial assembly of these features was often not "correct". We believe the reason for this behavior to be method-intrinsic, since the Bayesian classifier learned about the presence and absence of desirable features in a statistical fashion, but not primarily about the features' spatial arrangements. Here, fingerprints which consider larger inter-atomic distances within a molecule like the FCFP-12 fingerprint could potentially be of benefit.

The same reason might be true for the considerably higher selection rate of virtual hits coming from pharmacophore searching. Here, compounds like **14** and **23** were found to be "interesting" by medicinal chemists, possibly because the pharmacophoric pattern of the molecules matched better to what a human expert expects from years of research. Still, the number of actual in vitro hits was comparably low. This finding was primarily caused by poor compound solubility (data not shown). Several virtual hits could not be tested in our in vitro assay system because of precipitation. No initial estimation of physicochemical parameters like logP or logS was undertaken in this study, since we were determined on not to exclude any potential hit by additional computational constraints.

Only very few virtual hits from the shape search exhibit some in vitro activity. This finding is in accordance with the method's low performance in the retrospective validation. While some of the shape hits like **22** show basic similarity to known $Glycine_B$ reference compounds, many virtual hits were rather different to what one would expect from the known SAR. Still, we included the expert-selected molecules from shape searching as exploratory compounds to this study.

Finally, a high hit rate could be observed from molecular docking. While compounds **8** and **9** are highly similar to known reference structures, hits like **13** and **18** may be considered as novel. While we have found a high enrichment with known scaffolds among the Top 500 virtual docking hits (35%), we also observed the second-best acceptance rate by the medicinal chemist (21%). Apparently, the compounds suggested by molecular docking fulfilled required interaction constraints with the receptor and thus pharmacophoric points. At the same time, ligand-receptor shape complementarity seems to have biased the selection of virtual hits towards compounds with high shape similarity to the co-crystallized ligand DCKA from the X-ray structure we performed docking with. We believe the combination of these observations to be one possible reason for the comparably high hit rate of this method.

Conclusions

Two decades of research on the $Glycine_B$ site of the NMDA receptor have produced many potent ligands with high affinity, making it increasingly difficult to find new starting points for lead development in uncovered/unpatented chemical space. In this study, we have shown that it is still possible to identify novel, potentially unclaimed compounds with diverse scaffolds by applying several virtual screening techniques. We noticed considerable differences in the computation time required for different virtual screening experiments, but all methods presented

here were able to retrieve molecules with potentially novel scaffolds. Also, while some computationally demanding methods like 3D pharmacophore searching or molecular docking correctly identified a high percentage of true actives, the equally demanding shape search under-performed in this case. The comparably fast Bayesian classifier did not identify many structures which were subsequently selected for testing by the human expert, nevertheless a significant percentage of those compounds were true actives.

We also found that all methods presented were complementary, e.g. no molecule from the final hit list was identified by more than one virtual screening technique. It is thus worthwhile to exploit the full portfolio of available methods–computationally demanding and fast ones–in order not to miss out on potentially interesting structures.

Acknowledgments Dr. Manuela López de la Paz, Dr. Udo Meyer and Dr. Lutz Franke are thanked for valuable discussions. Swetlana Derksen is thanked for help in the compilation of literature references. The in vitro screening department at Merz Pharmaceuticals, especially Dr. Meik Sladek, Dr. Claudia Jatzke, Tanja Bauer and Christina Wollenburg are thanked for the in vitro screening of our compounds and stimulating and most helpful discussion.

References

1. Watkins JC, Evans RH (1981) Excitatory amino acid transmitters. Annu Rev Pharmacol Toxicol 21(1):165–204
2. Nowak L, Bregestovski P, Ascher P, Herbet A, Prochiantz A (1984) Magnesium gates glutamate-activated channels in mouse central neurones. Nature 307(5950):462–465
3. Cull-Candy SG, Usowicz MM (1987) Multiple-conductance channels activated by excitatory amino acids in cerebellar neurons. Nature 325(6104):525–528
4. Jahr CE, Stevens CF (1987) Glutamate activates multiple single channel conductances in hippocampal neurons. Nature 325(6104): 522–525
5. Moriyoshi K, Masu M, Ishii T, Shigemoto R, Mizuno N, Nakanishi S (1991) Molecular cloning and characterization of the rat NMDA receptor. Nature 354(6348):31–37
6. Greenamyre JT, O'Brien CF (1991) N-methyl-D-aspartate antagonists in the treatment of Parkinson's disease. Arch Neurol 48(9):977–981
7. Geddes JW, Chang-Chui H, Cooper SM, Lott IT, Cotman CW (1986) Density and distribution of NMDA receptors in the human hippocampus in Alzheimer's disease. Brain Res 399(1):156–161
8. Danysz W, Parsons C (2003) The NMDA receptor antagonist memantine as a symptomatological and neuroprotective treatment for Alzheimer's disease: preclinical evidence. Int J Geriatr Psychiatry 18(S1):S23–S32
9. Olney J (1999) NMDA receptor hypofunction model of schizophrenia. J Psychiatr Res 33(6):523–533
10. Laube B, Kuhse J, Betz H (1998) Evidence for a tetrameric structure of recombinant NMDA receptors. J Neurosci 18(8): 2954–2961
11. Furukawa H, Singh S, Mancusso R, Gouaux E (2003) Subunit arrangement and function in NMDA receptors. Nature 438(7065): 185–192
12. Kleckner NW, Dingledine R (1988) Requirement for glycine in activation of NMDA-receptors expressed in Xenopus oocytes. Science 241(4867):835–837
13. Laube B, Hirai H, Sturgess M, Betz H, Kuhse J (1997) Molecular determinants of agonist discrimination by NMDA receptor subunits: analysis of the glutamate binding site on the NR2B subunit. Neuron 18(3):493–503
14. Danysz W, Parsons CG (1998) GlycineB recognition site of NMDA receptors and its antagonists. Amino Acids 14(1–3):205–206
15. Simon RP, Swan JH, Griffiths T, Meldrum BS (1984) Blockade of N-methyl-D-aspartate receptors may protect against ischemic damage in the brain. Science 226(4676):850–852
16. Parsons C (2001) NMDA receptors as targets for drug action in neuropathic pain. Eur J Pharmacol 429(1–3):71–78
17. Oprea TI (2000) Current trends in lead discovery: are we looking for the appropriate properties? Mol Divers 5(4):199–208
18. Schneider G, Neidhart W, Giller T, Schmid G (1999) "Scaffold-hopping" by topological pharmacophore search: a contribution to virtual screening. Angew Chem Int Ed 38(19):2894–2896
19. Schneider G, Schneider P, Renner S (2006) Scaffold-hopping: how far can you jump? QSAR Comb Sci 25(12):1162–1171
20. Lipinski C, Hopkins A (2004) Navigating chemical space for biology and medicine. Nature 432(7019):855–861
21. Dobson C (2004) Chemical space and biology. Nature 432(7019): 824–828
22. Hertzberg RP, Pope AJ (2000) High-throughput screening: new technology for the 21st century. Curr Opin Chem Biol 4(4): 445–451
23. Silverman L (1998) New assay technologies for high-throughput screening. Curr Opin Chem Biol 2(3):397–403
24. Gribbon P, Sewing A (2005) High-throughput drug discovery: what can we expect from HTS? Drug Discovery Today 10(1):17–22
25. Schneider G (2002) Trends in virtual combinatorial library design. Curr Med Chem 9(23):2095–2101
26. Leach A (2000) The in silico world of virtual libraries. Drug Discovery Today 5(8):326–336
27. Van Drie J (1998) Approaches to virtual library design. Drug Discovery Today 3(6):274–283
28. Jenkins JL, Kao RYT, Shapiro R (2003) Virtual screening to enrich hit lists from high-throughput screening: A case study on small-molecule inhibitors of angiogenin. Proteins 50(1):81–93
29. Olah M, Mracec M, Ostopovici L, Rad R, Bora A, Hadaruga N, Olah I, Banda M, Simon Z, Mracec M, Oprea TI (2004) WOMBAT: world of molecular bioactivity. Chemoinformatics in Drug Discovery 223–239
30. Walters WP, Stahl MT, Murcko MA (1998) Virtual screening–an overview. Drug Discov Today 3:160–178
31. Hann M, Hudson B, Lewell X, Lifely R, Miller L, Ramsden N (1999) Strategic pooling of compounds for high-throughput screening. J Chem Inf Comput Sci 39(5):897–902
32. Weininger D (1988) SMILES, a chemical language and information system. 1. Introduction to methodology and encoding rules. J Chem Inf Comput Sci 28(1):31–36
33. Weininger D, Weininger A, Weininger J (1989) SMILES. 2. Algorithm for generation of unique SMILES notation. J Chem Inf Comput Sci 29(2):97–101
34. Lipinski C, Lombardo F, Dominy B, Feeney P (2001) Experimental and computational approaches to estimate solubility and permeability in drug discovery and development settings. Adv Drug Deliv Rev 46(1–3):3–26
35. Lipinski C (2004) Lead- and drug-like compounds: the rule-of-five revolution. Drug Discov Today Technol 1(4):337–341
36. Snarey M, Terrett N, Willett P, Wilton D (1997) Comparison of algorithms for dissimilarity-based compound selection. J Mol Graph Model 15(6):372–385

37. Hanley J, McNeil B (1983) A method of comparing the areas under receiver operating characteristic curves derived from the same cases. Radiology 148(3):839–843
38. Zou KH, O'Malley AJ, Mauri L (2007) Receiver-operating characteristic analysis for evaluating diagnostic tests and predictive models. Circulation 115(5):654–657
39. Matthews BW (1968) Solvent content of protein crystals. J Mol Biol 33(2):491–497
40. Bernardo J, Smith A (2001) Bayesian theory. Meas Sci Technol 12(2):221–222
41. Cheng MH, Coalson RD, Cascio M (2007) Molecular dynamics simulations of ethanol binding to the transmembrane domain of the glycine receptor: Implications for the channel potentiation mechanism. Proteins 71(2):972–981
42. Xia X, Maliski EG, Gallant P, Rogers D (2004) Classification of kinase inhibitors using a Bayesian model. J Med Chem 47(18):4463–4470
43. Klon AE, Lowrie JF, Diller DJ (2006) Improved naive bayesian modeling of numerical data for absorption, distribution, metabolism and excretion (ADME) property prediction. J Chem Inf Model 46(5):1945–1956
44. Rogers D, Brown R, Hahn M (2005) Using extended-connectivity fingerprints with laplacian-modified bayesian analysis in high-throughput screening follow-up. J Biomol Screen 10(7):682–686
45. Liu Y (2004) A comparative study on feature selection methods for drug discovery. J Chem Inf Comput Sci 44(5):1823–1828
46. Vogt M, Bajorath J (2008) Bayesian screening for active compounds in high-dimensional chemical spaces combining property descriptors and molecular fingerprints. Chem Biol Drug Des 71(1):8–14
47. Poschenrieder H, Stachel H, Hofner G, Mayer P (2005) Novel pyrrolinones as N-methyl-D-aspartate receptor antagonists. Eur J Med Chem 40(4):391–400
48. Guzikowski A (1995) 6, 7, 8, 9-tetrahydro-3-hydroxy-1H–1-benzazepine-2, 5-diones via a diels-alder reaction: antagonists with a non-planar hydrophobic region for NMDA receptor glycine sites. Bioorg Med Chem Lett 5(22):2747–2748
49. Varano F, Catarzi D, Colotta V, Filacchioni G, Galli A, Costagli C, Carla V (2002) Synthesis and biological evaluation of a new set of pyrazolo[1, 5-c]quinazoline-2-carboxylates as novel excitatory amino acid antagonists. J Med Chem 45(5):1035–1044
50. MacLeod AM, Grimwood S, Barton C, Bristow L, Saywell KL, Marshall GR, Ball RG (1995) Identification of 3, 5-Dihydro-2-aryl-1H-pyrazolo[3, 4-c]quinoline-1, 4(2H)-diones as novel high-affinity glycine site N-methyl-D-aspartate antagonists. J Med Chem 38(12):2239–2243
51. Baron BM, Cregge RJ, Farr RA, Friedrich D, Gross RS, Harrison BL, Janowick DA, Matthews D, McCloskey TC, Meikrantz S, Nyce PL, Vaz R, Metz WA (2005) CoMFA, Synthesis, and Pharmacological Evaluation of (E)-3-(2-Carboxy-2-arylvinyl)-4, 6-dichloro-1H-indole-2-carboxylic Acids: 3-[2-(3-Aminophenyl)-2-carboxyvinyl]-4, 6-dichloro-1H-indole-2-carboxylic Acid, a Potent Selective Glycine-Site NMDA Receptor Antagonist. J Med Chem 48(4):995–1018
52. Leeson PD, Carling RW, Moore KW, Moseley AM, Smith JD, Stevenson G, Chan T, Baker R, Foster AC (1992) 4-Amido-2-carboxytetrahydroquinolines Structure-activity relationships for antagonism at the glycine site of the NMDA receptor. J Med Chem 35(11):1954–1968
53. Berman HM, Westbrook J, Feng Z, Gilliland G, Bhat TN, Weissig H, Shindyalov IN, Bourne PE (2000) The protein data bank. Nucleic Acids Res 28(1):235–242
54. Furukawa H, Gouaux E (2003) Mechanisms of activation, inhibition and specificity: crystal structures of the NMDA receptor NR1 ligand-binding core. EMBO J 22(12):2873–2885
55. Inanobe A, Furukawa H, Gouaux E (2005) Mechanism of partial agonist action at the NR1 subunit of NMDA receptors. Neuron 47(1):71–84
56. Pentikainen U, Settimo L, Johnson M, Pentikainen O (2006) Subtype selectivity and flexibility of ionotropic glutamate receptors upon antagonist ligand binding. Org Biomol Chem 4(6): 1058–1070
57. Kaye SL, Sansom MS, Biggin PC (2006) Molecular dynamics simulations of the ligand-binding domain of an N-methyl-D-aspartate receptor. J Biol Chem 281(18):12736–12742
58. Jorgensen W, Tirado-Rives J (1988) The OPLS [optimized potentials for liquid simulations] potential functions for proteins, energy minimizations for crystals of cyclic peptides and crambin. J Am Chem Soc 110(6):1657–1666
59. Friesner RA, Banks JL, Murphy RB, Halgren TA, Klicic JJ, Mainz DT, Repasky MP, Knoll EH, Shelley M, Perry JK, Shaw DE, Francis P, Shenkin PS (2004) Glide: a new approach for rapid, accurate docking and scoring. 1. Method and assessment of docking accuracy. J Med Chem 47(7):1739–1749
60. Halgren TA, Murphy RB, Friesner RA, Beard HS, Frye LL, Pollard WT, Banks JL (2004) Glide: a new approach for rapid, accurate docking and scoring. 2. Enrichment factors in database screening. J Med Chem 47(7):1750–1759
61. Friesner RA, Murphy RB, Repasky MP, Frye LL, Greenwood JR, Halgren TA, Sanschagrin PC, Mainz DT (2006) Extra precision glide: docking and scoring incorporating a model of hydrophobic enclosure for protein-ligand complexes. J Med Chem 49(21): 6177–6196
62. Hawkins P, Warren G, Skillman A, Nicholls A (2008) How to do an evaluation: pitfalls and traps. J Comput Aided Mol Des 22(3–4): 179–190
63. Wold S, Ruhe A, Wold H, Dunn WJ (1984) The collinearity problem in linear regression. The partial least squares (PLS) approach to generalized inverses. SIAM J Sci Stat Comput 5(3): 735–743
64. Wold H (ed) (1985) Systems analysis by partial least squares. Martinus Nijhoff, Boston
65. Hawkins PCD, Skillman AG, Nicholls A (2007) Comparison of shape-matching and docking as virtual screening tools. J Med Chem 50(1):74–82
66. Proschak E, Rupp M, Derksen S, Schneider G (2008) Shapelets: possibilities and limitations of shape-based virtual screening. J Comput Chem 29(1):108–114
67. Dannhardt G, von Gruchalla M, Kohl BK, Parsons CG (2000) A novel series of 2-carboxytetrahydroquinolines provides new insights into the eastern region of glycine site NMDA antagonists. Arch Pharm (Weinheim) 333(8):267–274
68. Fray MJ, Bull DJ, Carr CL, Gautier ECL, Mowbray CE, Stobie A (2001) Structure-activity relationships of 1, 4-dihydro-(1H, 4H)-quinoxaline-2, 3-diones as N-methyl-D-aspartate (glycine site) receptor antagonists. 1. Heterocyclic substituted 5-alkyl derivatives. J Med Chem 44(12):1951–1962
69. Baron B, Siegel B, Harrison B, Gross R, Hawes C, Towers P (1996) [3H]MDL 105, 519, a high-affinity radioligand for the N-methyl-D-aspartate receptor-associated glycine recognition site. J Pharmacol Exp Ther 279(1):62–68